Biomaterials 95 (2016) 22–34

Contents lists available at ScienceDirect

Biomaterials

journal homepage: www.elsevier.com/locate/biomaterials

Nanolayered siRNA delivery platforms for local silencing of CTGF reduce cutaneous scar contraction in third-degree burns

Steven A. Castleberry [a, b, c, d], Alexander Golberg [e, f], Malak Abu Sharkh [a], Saiqa Khan [g], Benjamin D. Almquist [a, b, c], William G. Austen Jr. [g], Martin L. Yarmush [e, h], Paula T. Hammond [a, b, c, *]

[a] Department of Chemical Engineering, Massachusetts Institute of Technology, Cambridge, MA, 02139, USA
[b] Koch Institute of Integrative Cancer Research, Massachusetts Institute of Technology, Cambridge, MA, 02139, USA
[c] Institute for Soldier Nanotechnologies, Massachusetts Institute of Technology, Cambridge, MA, 02139, USA
[d] Harvard-MIT Division of Health Sciences and Technology, Cambridge, MA, 02139, USA
[e] Center for Engineering in Medicine, Department of Surgery, Massachusetts General Hospital, Harvard Medical School, and the Shriners Burns Hospital, Boston, MA, 02114, USA
[f] Porter School of Environmental Studies, Tel Aviv University, Ramat-Aviv, Tel Aviv, Israel
[g] Division of Plastic and Reconstructive Surgery, Massachusetts General Hospital, Harvard Medical School, Boston, MA, 02114, USA
[h] Department of Biomedical Engineering, Rutgers University, Piscataway, NJ, 08901, USA

ARTICLE INFO

Article history:
Received 30 January 2016
Received in revised form
6 April 2016
Accepted 10 April 2016
Available online 14 April 2016

Keywords:
siRNA delivery
Controlled release
CTGF
Scar formation
Layer-by-layer
Wound healing

ABSTRACT

Wound healing is an incredibly complex biological process that often results in thickened collagen-enriched healed tissue called scar. Cutaneous scars lack many functional structures of the skin such as hair follicles, sweat glands, and papillae. The absence of these structures contributes to a number of the long-term morbidities of wound healing, including loss of function for tissues, increased risk of re-injury, and aesthetic complications. Scar formation is a pervasive factor in our daily lives; however, in the case of serious traumatic injury, scars can create long-lasting complications due to contraction and poor tissue remodeling. Within this report we target the expression of connective tissue growth factor (CTGF), a key mediator of TGFβ pro-fibrotic response in cutaneous wound healing, with controlled local delivery of RNA interference. Through this work we describe both a thorough *in vitro* analysis of nanolayer coated sutures for the controlled delivery of siRNA and its application to improve scar outcomes in a third-degree burn induced scar model in rats. We demonstrate that the knockdown of CTGF significantly altered the local expression of αSMA, TIMP1, and Col1a1, which are known to play roles in scar formation. The knockdown of CTGF within the healing burn wounds resulted in improved tissue remodeling, reduced scar contraction, and the regeneration of papillary structures within the healing tissue. This work adds support to a number of previous reports that indicate CTGF as a potential therapeutic target for fibrosis. Additionally, we believe that the controlled local delivery of siRNA from ultrathin polymer coatings described within this work is a promising approach in RNA interference that could be applied in developing improved cancer therapies, regenerative medicine, and fundamental scientific research.

1. Introduction

Wound healing is an incredibly complex process involving the orchestration of numerous cytokines, cell types, and biological pathways in response to injury [4]. Scar formation as a result of wound healing impacts the life of almost every patient with a wound, ranging from serious trauma to plastic surgery to even playground roughhousing. Scars can detrimentally impact a patient's quality of life [1–3]. Importantly, scar formation from serious trauma can often be debilitating by reducing range of motion and joint mobility and subsequently impairing function [4–6]. The current treatment options for scars offers little comfort for patients, often consisting of topical steroids which have serious undesirable

* Corresponding author. Department of Chemical Engineering, Koch Institute of Integrative Cancer Research, Massachusetts Institute of Technology, Room 76-553, Cambridge, MA, 02139, USA.
E-mail address: hammond@mit.edu (P.T. Hammond).

http://dx.doi.org/10.1016/j.biomaterials.2016.04.007
0142-9612/

side-effects, surgical resection which has a low success rate and a considerable risk of infection, and simple silicone-based gel wraps [7,8].

The goal of normal cutaneous wound healing is to regenerate the naturally protective structures of the skin quickly so as to reduce the risk of infection and provide functioning tissue [9–11]. This process is made up of a number of different stages, including hemostasis, inflammation, proliferation, and remodeling [12]. The last two of these stages, proliferation and remodeling, are especially important in determining scar formation as they pertain to the production of the healing extracellular matrix (ECM) and its reorganization [13–16]. In scarring, this healing process does not regenerate all of the native structures of the skin, leaving a poorly organized dense collagen-rich matrix that is often highly contracted by myofibroblasts [2,17–19]. This is often the case in hypertrophic scarring, which can result from traumatic injuries such as blast or burn wounds [20–23].

Because scarring is such an ever-present occurrence in daily life, a great deal of research has been focused on understanding the underlying pathologic causes for it. Much of this research has focused on the dysregulated signaling of transforming growth factor-beta (TGFβ) within wounds [15,24–28], as it has been shown that upregulated expression of TGFβ is correlated to increased fibrosis in animal models of cutaneous scarring [14,29–33]. Proper signaling of TGFβ within wounds, however, is necessary for healthy wound healing, as it orchestrates a number of disparate pathways integral in effective tissue regeneration and remediation of inflammation [24,27,34]. To this end it has been demonstrated that the inhibition of TGFβ *in vivo* significantly reduces scar formation but also greatly impairs wound healing [35]. For this reason efforts to target TGFβ signaling directly raise concerns about the total impact of such therapies.

Connective tissue growth factor (CTGF) is a key downstream mediator of TGFβ signaling that has been demonstrated to regulate many of its pro-fibrotic effects [36–43]. CTGF has been shown to play an important role in regulating many key cellular processes within wound healing, including cell proliferation and migration as well as myofibroblast differentiation and ECM production [39–41,44,45]. CTGF also functions to assist in TGFβ-based stimulation of collagen and tissue inhibitor of metalloprotenase-1 (TIMP-1) expression [46–49]. A number of previous reports have described the potentially pathologic overexpression of CTGF within fibrotic diseases, including dermal scarring, where its increased expression has been well-characterized within keloids [46,50–53].

As CTGF has been demonstrated to function as a key mediator of scar formation *in vivo*, targeting its expression as a means of reducing scar formation is logical [25,26,30,54,55]. Previous research has demonstrated some success in this approach using anti-sense RNA therapy; however, these approaches have focused on direct bolus injection of un-encapsulated siRNA [56–60]. This leaves the delivered siRNA open to rapid degradation and clearance from the target tissue, significantly reducing its efficacy. Even with these drawbacks, these reports have demonstrated significant siRNA-specific reduction in CTGF expression leading to substantial changes in scar formation. This literature, as a whole, builds a compelling case for targeted anti-CTGF therapies in the treatment of scar production, but also provides evidence for the need to develop more effective techniques for controlled siRNA delivery.

We have previously described the use of layer-by-layer (LbL) [61–65] assembly to construct ultrathin polymer films for the controlled localized delivery of siRNA into chronic wounds to significantly accelerate wound healing *in vivo*. These reports have focused on the delivery of siRNA from a commercially available woven nylon bandage applied directly into healing wounds. To apply this technology to anti-scar therapy, it is first imperative that an adequate animal model be chosen in which scarring behavior can be observed. We chose to conduct this research in a rat third-degree burn model as it has been demonstrated to form highly reproducible scars [66–68], and burn wounds are known to overexpress CTGF [69,70]. Burn scars, however, do not present open wounds, as is the case for excisional models, thus requiring us to make adjustments to the substrate coated for implantation into the healing burn wound. For this purpose, we used a commercially available silk suture which provided a mechanically robust substrate. Coating sutures for anti-scar therapy has the added benefit of being widely applicable in the arena of scar therapy, as many scars are the result of surgical procedures or traumatic injury, where sutures would already be used. We note that here we use a commonly used silk suture, but the same electrostatic assembly approach described here can be applied to synthetic and fully resorbable suture materials with appropriate surface treatment.

In this work we describe the application of an ultrathin polymer film coating generated from a simple encapsulation method of electrostatic multilayer assembly, and applied to a commercially available suture for the controlled local delivery of siRNA into healing third-degree burns. This coating was first thoroughly investigated *in vitro* to demonstrate efficacy of siRNA delivery from the coated substrate, achieving sustained levels of siRNA-specific gene knockdown for up to five days with a controlled siRNA release profile. The coated sutures were directly placed into healing burns on the dorsum of rats and produced significant siRNA-specific reductions in targeted gene expression. The controlled knockdown of CTGF within the healing burns resulted in greatly reduced scar contraction, improved tissue remodeling, and the regeneration of important native tissue structures such as papillae which are lost in all other burn control groups.

2. Methods and materials

2.1. Materials

Poly 2 (20 kDa) was synthesized as previously reported [71]. Chitosan (15 kDa) and dextran sulfate (500 kDa) were purchased from Sigma Aldrich company (Manassas, VA). SiRNA sequences were synthesized by Dharmacon (Lafayette, CO); alexafluor 488-labeled and 546-labeled siRNA was purchased from Qiagen (Valencia, CA). Ethicon 4-0 Perma-Hand Silk suture were purchased from Santa Cruz Biotechnology Inc. (Dallas, TX). Phosphate-buffered saline (PBS, 10x), Advanced-MEM, fetal bovine serum, antibiotic-antimycotic solution, and 100 mM L-Glutamine solution were purchased from Invitrogen (Carlsbad, CA). NIH-3T3, HeLa, and MDA-MB-231 cells were purchased from Cell Biolabs (San Diego, CA). All antibodies were purchased from Abcam (Cambridge, MA).

2.2. Layer-by-layer film preparation

Films were deposited on oxygen plasma treated sutures. Sutures were cleaned in ethanol and then in RNase free UltraPure™ water (Life Technologies) prior to plasma treatment. Oxygen plasma treatment was performed for 3 min on high setting. Sutures were then immediately immersed in a solution of the polycation Poly 2 for a minimum of 1 h. Assembly of LbL films was performed using a Carl Zeiss HMS-DS50 stainer. [Poly 2/DS] base layers were deposited through sequential polymer adsorption steps (2 mg ml^{-1}, pH 5.0) of 10 min. Between each polymer deposition step the bandages were washed twice in RNase free water (pH 5.0). Assembly of [CHI/siRNA] film was deposited similarly. Chitosan (1 mg ml^{-1}, pH 5.0) was adsorbed for 10 min and siRNA (20 μg ml^{-1}, pH 5.0) was adsorbed for 15 min. All solutions were prepared in RNase free water, adjusted to a pH of 5.0.

Film growth was characterized for films built on silicon wafers by a Veeco Dektak 150 profilometer. Incorporation of fluorescently labeled siRNA into films built on silk sutures was followed using a Nikon A1R Ultra-Fast Spectral Scanning confocal microscope. Total siRNA incorporation within films was measured by rapid dissolution in a 1 M NaCl solution with vigorous agitation for films assembled on sutures and quantified using a fluorescent plate reader. Release studies were performed in PBS (pH 7.4, 37 °C) and in cell conditioned media (37 °C). Release was quantified by fluorescence of the released labeled siRNA read using a fluorescent plate reader.

2.3. In vitro LbL bandage evaluation

Cells were cultured in Advanced-MEM media with 5% FBS, 1% antibiotic-antimycotic, and 2 mM L-glutamine. Cells were seeded at an initial density of 5000 cells per well in a 48-well plate. After one day LbL coated sutures (3 cm, cut to 1 cm lengths) were placed in culture with the cells. The suture coatings either contained GFP-specific siRNA or a control siRNA sequence or were uncoated. Uncoated suture was used as the control to test the cytotoxicity of the film. Mean cell fluorescence was measured by flow cytometry, using a BD FACSCalibur flow cytometer. Cell viability was quantified using AlamarBlue assay (Life Technologies). Analysis of GFP expression and cell viability were performed after 3 and 5 days of treatment.

2.4. In vivo siRNA delivery

All animal studies were approved by the MIT Institutional Animal Care and Use Committee (IACUC) and by the Subcommittee on Research Animal Care (IACUC) of the Massachusetts General Hospital. Animals were housed and cared for in the USDA-inspected MIT Animal Facility under federal, state, local, and NIH guidelines for animal care. Six week old Sprague-Dawley rats (~200 g, n = 3) were purchased from Charles River Laboratories (Wilmington, MA). Three groups of sutures were used: (1) CTGF siRNA (siCTGF) suture treated, (2) control siRNA (siControl) suture treated, and (3) uncoated suture treated.

Prior to wounding, rats were anesthetized with isoflurane. Hair was removed from the backs of rats using an electric clipper. Six burn wounds were created on the dorsum of each rat by applying the end of a pre-heated brass block (≥95 °C) for 10 s. Each wound was created with a single application of a pre-heated brass block. This protocol results in a non-lethal, full-thickness, third-degree burn measuring approximately 1 cm [2]. Burns were spaced evenly down the midline of the rat starting from the top of the back and going down to 2 cm above the tail. Each rat received all three treatments, with two burn wounds of each treatment type per rat. Sutures were placed immediately after burn creation. They were placed running laterally across the burn in a vertical mattress suture, with four total passes through each burn. Sutures were placed through the dermis so as to not impair skin movement. Digital imaging of burns was performed after 15 and 30 days of treatment. Rats were sacrificed after 30 days. Each wound was cut so tissue for RNA isolation was taken from the treated scar. These wounds were then used for histological analysis.

2.5. Histology

Tissues were fixed in zinc fixative without formalin for 48 h. The excised wounds were cut on center and then embedded cut-face down in paraffin. Sections were taken at the wound center and at two further levels of 250 μm reaching a total of 1 mm sampling length through the scar. At each level a hematoxylin and eosin (H&E) slide was stained. Unstained slides were also taken for IHC, MTC, and PS staining and analysis of the healing tissue. All sections were 5 μm thick. Image analysis was performed using Image J. Orientation of collagen fibers was analyzed using the Image J plugin Orientation J.

2.6. Tissue processing

Isolation of RNA was performed using TRIzol as per the manufacturer's instructions. Synthesis of cDNA was done using iScript cDNA synthesis kit (Bio-Rad Laboratories) and analysis of expression was performed by qRT-PCR using iQ SYBR Green Supermix (Bio-Rad Laboratories) along with selected DNA primer pairs. All experiments were performed in triplicate using a LightCycler 480 (Roche). Relative gene expression was quantified relative to β-actin, a housekeeping gene, using the delta-delta Ct method.

2.7. Statistics

Statistical analysis was performed between groups using Student's *t*-test and rectified by ANOVA for comparisons between multiple groups. Values are represented as mean ± S.D. A value of $p < 0.05$ was used to indicate statistical significance.

3. Results

The film used in this work consists of a hierarchical structure of two simple bilayer LbL films. The first film applied to the surface is a hydrolytically degradable film using Poly2, a poly(beta-aminoester), and dextran sulfate (Fig. 1a). This undercoating film forms a hydrolytically erodible base on which the later film is assembled. On top of this film the siRNA incorporating layer of low molecular weight chitosan and siRNA are applied (Fig. 1b). This combinatory film structure has the capability to both incorporate siRNA and release the assembled film material from the coated surface.

Here we investigate the application of this film architecture to deliver siRNA into healing burn wounds for scar remediation. As layer-by-layer assembly is an equilibrium driven process that has been reported to be effectively reproducible on a variety of surfaces we began our work by demonstrating this feature of the LbL assembly. Films were assembled on cleaned silk suture, as described in the methods section of this work, that were oxygen plasma treated on high for 3 min. Films were assembled as previously described. Total film incorporation of siRNA was evaluated based on a per centimeter length basis.

3.1. Evaluation of LbL film coating on silk sutures

It was observed that siRNA incorporation on the suture was near-linear with the number of siRNA containing layers, similar to what had been observed for coated nylon bandage and silicon substrates (Fig. 2a) [72]. When 25 layers of the [Chi/siRNA] film were assembled onto a $[Poly2/DS]_{20}$ coated suture, a total of 2.1 ± 0.3 μg/cm of siRNA was incorporated. We evaluated the release of the siRNA from this coated surface in two different release media. The first was PBS at 7.4 and 37 °C, which is a common release media for degradable delivery systems, as it effectively reproduces the body's salt concentration and pH. PBS, however, does not capture the biological protein interactions that may also contribute in facilitating material release. To better estimate release in biologic media we used cell conditioned media at 37 °C, as described in the methods and materials section of this report.

Film coated sutures in cell conditioned media were observed to sustain the release of siRNA for over nine days, while the PBS media

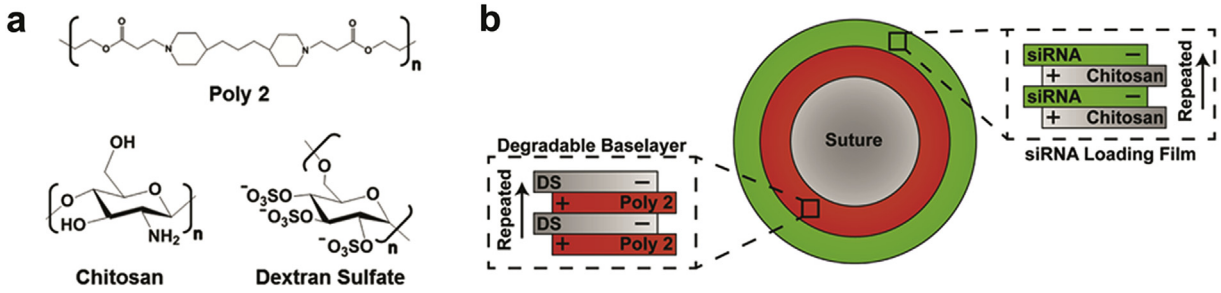

Fig. 1. Layer-by-layer film architecture for the controlled local delivery of siRNA. (a) Chemical structure of repeating unit of polymers used in film assembly. (b) Schematic cartoon of LbL assembly as constructed on the suture surface.

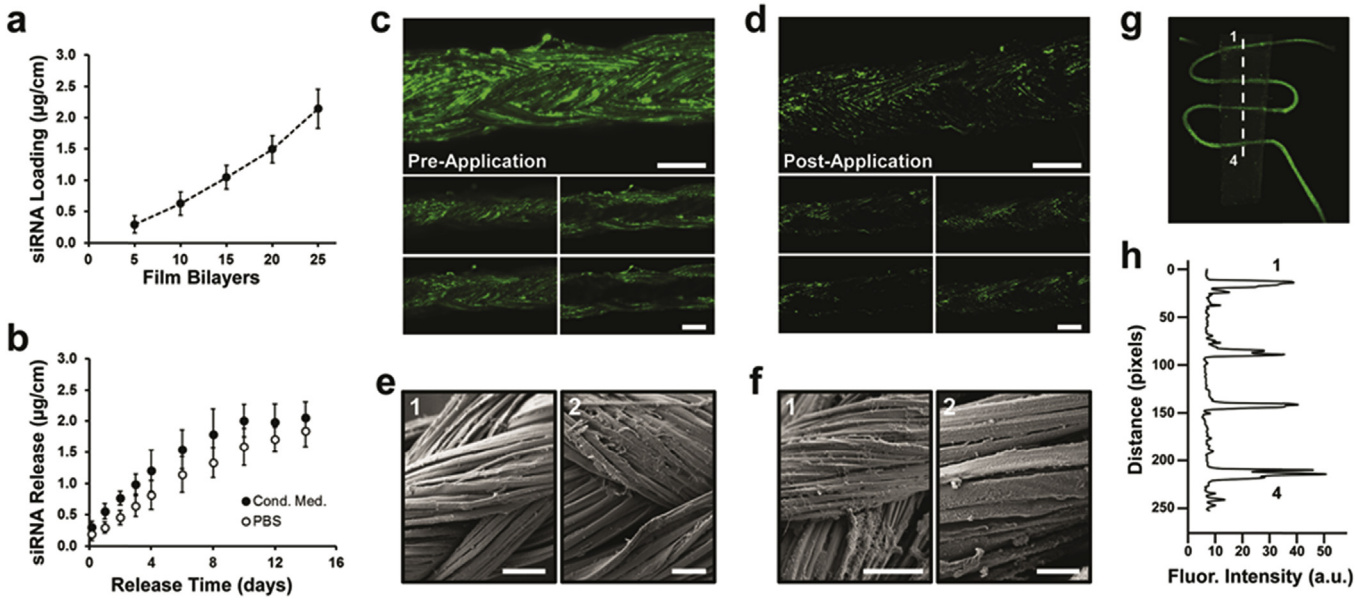

Fig. 2. *In vitro* characterization of LbL coating applied to a commercially available silk suture. (a) siRNA incorporation per cm of coated suture at 5, 10, 15, 20, and 25 architecture repeats. (b) Release of siRNA over 14 days *in vitro* in either PBS or cell conditioned media at 37 °C. (c) Confocal imaging of fluorescently labeled siRNA incorporated within the film coating prior to degradation. (d) Confocal imaging of fluorescently labeled siRNA incorporated within the film coating five days into degradation in cell conditioned media. (e) SEM images of LbL coated silk suture prior to degradation. Scale bar = 100 μm (1), 25 μm (2). (f) SEM images of LbL coated silk suture after five days degradation in cell conditioned media. Scale bar = 100 μm (1), 15 μm (2). (g) LbL coated silk suture drawn through polydimethylsiloxane (PDMS) block and then imaged using a Typhoon 9400 Variable Mode Imager. The number of times the suture has passed through the block is marked from 1 to 4. (h) Quantification of relative fluorescent signal along the dashed line in (g) with locations 1 and 4 marked as such. Data shown are mean ± S.D., n = 3.

resulted in release carried out to nearly 12 days, as shown in Fig. 2b. These findings suggest an impact of release media on the release of the siRNA, likely due to the interactions of charged proteins that compete with the ionic crosslinks that form films. This release was followed using a fluorescently labeled siRNA, imaging of the film coating the suture containing the labeled siRNA prior to release is shown in Fig. 2c. The coating is observed to uniformly cover the surface of the woven silk suture with only a few defects observed. A few punctate localizations of fluorescent signal are observed in the coating, primarily lying in the recesses between individual fibers. This is likely aggregation of the accumulating film material between the fibers. After seven days of degradation in the cell conditioned media much of the labeled siRNA is observed to be released from the surface (Fig. 2d). This release is observed to occur in patches across the coated surface. Large areas of fluorescence are still apparent after the seven days of degradation, but the total level of fluorescence is seen to be significantly reduced.

Scanning electron micrograph (SEM) images of film-coated sutures demonstrate the uniform level of coating across the suture. A few areas of bridging are visible across the woven network of fibers (Fig. 2e2), but the individual fibers are still apparent upon observation (Fig. 2e1). SEM images of the coated suture after seven days of degradation in cell conditioned media showed significant degradation of the coating surface. Many noticeable defects are observed along the surface of the coated fibers, with the fibers appearing to have pieces of swollen film crossing between them (Fig. 2f1). Close examination of the fibers shows an increasingly rough surface with noticeable flaking off of the coating (Fig. 2f2).

The LbL coating on the suture after assembly appeared uniform over the surface; however, adhesion of the film to the suture during its use was a concern, as it would lead to loss of siRNA from the surface. To investigate this potential issue, we assembled the LbL film on the surface of the silk suture containing a labeled siRNA and drew the suture through a PDMS block four times (Fig. 2g). We then imaged the suture *in situ* to evaluate the level of remaining fluorescent material on the suture (Fig. 2h). What we observed was little to no detrimental loss of the labeled signal from the suture after being drawn though the PDMS. We repeated this test using excised pig dermis and observed a similar phenomenon when we compared fresh suture to that which had been drawn through the

skin four times. These findings lend support to the application of such a suture *in vivo*, as the material assembled on the fiber surface is expected to remain on the suture at the site of implantation.

3.2. In vitro investigation of siRNA delivery from LbL coated sutures

We next wanted to investigate the activity of the incorporated siRNA. To do this placed 3 cm of the coated suture into culture with cells expressing the reporter gene green fluorescent protein (GFP). The sutures were cut to 1 cm long lengths and were allowed to settle in the wells. We were particularly careful in the slow and deliberate even placement of the cut suture throughout the well to avoid issues such as non-uniform release to cells. *In vitro* studies for the knockdown of the GFP were carried out in two cell lines, HeLa and NIH-3T3 that constitutively express GFP. After three days of treatment significant siRNA-specific gene knockdown was observed in both cell lines. GFP reduction after three days was approximately 37% in HeLa cells and 31% in NIH-3T3 cells. This knockdown was observed to increase at five days to nearly 55% in HeLa cells and 48% in NIH-3T3 cells (Fig. 3a). No significant cytotoxicity was observed for the LbL coated sutures versus sutures that were as purchased (Fig. 3b). Importantly, no proximity related cell changes were observed for cells in culture close to the sutures. This was evaluated by brightfield and fluorescent imaging of cells at varied distances from siRNA delivering sutures.

Uptake of the labeled siRNA in HeLA cells was observed to increase during the five day testing period. Large micron sized particles were seen to accumulate around cells while more diffusely labeled sub-micron localizations were observed intracellular (Fig. 3c–d). The level of diffuse labeling within the cells increased from day three to day five. This pattern fits well with our imaging studies of the releasing LbL coated suture, as we can clearly visualize these multi-micron sized particles flaking off of the coated surface as the film breaks up during the release process.

3.3. In vivo application of LbL coated sutures

Six week old Sprague-Dawley rats were prepared for surgery under anesthesia. The dorsum of each rat was shaven with an electric clipper and cleaned immediately prior to wounding. Burn wounds were created along the midline of the dorsum using heated (≥95 °C) brass blocks (Fig. 4c) applied to the skin of the rat for 10 s. Wounds were created evenly down the back of each rat starting at the top of the back and ending approximately 2 cm above the tail. Sutures were placed through each burn wound laterally crossing the burn four times in a vertical mattress suture style. The excess suture was clipped near the skin surface leaving as little as possible for the rat to interact with. Sutures were placed such that they ran through the scar dermis but entered and exited through the uninjured margins approximately 1–2 mm outside of the burn wound at either margin (Fig. 4a).

The wounding and suture placement was carried out as described in Fig. 4a and resulted in a well reproducible model where rats are largely unable to interfere with their sutured burns and the sutures remain intact within the burn wounds (Fig. 4b). Throughout the one month study, we did not observe any removal of suture by the rats, and the sutures appeared well tolerated with only limited discomfort noticed in the first few days after wounding. Suture placement is important in this model, as the wounded tissue will quickly become necrotic and lose much of its mechanical stability. This wounded tissue is known to fall off of the burn wounds after approximately two weeks, and thus, care was taken to ensure that sutures did not exit the dermis inside of the burn tissue area, where they would have been much easier for the rat to remove. Wounds were treated with one of three types of suture: (1) siCTGF, (2) siControl, and (3) uncoated. Each rat had two wounds treated with each type of suture. Suture location along the back was changed for each rat to control for potential differences in contraction along the back.

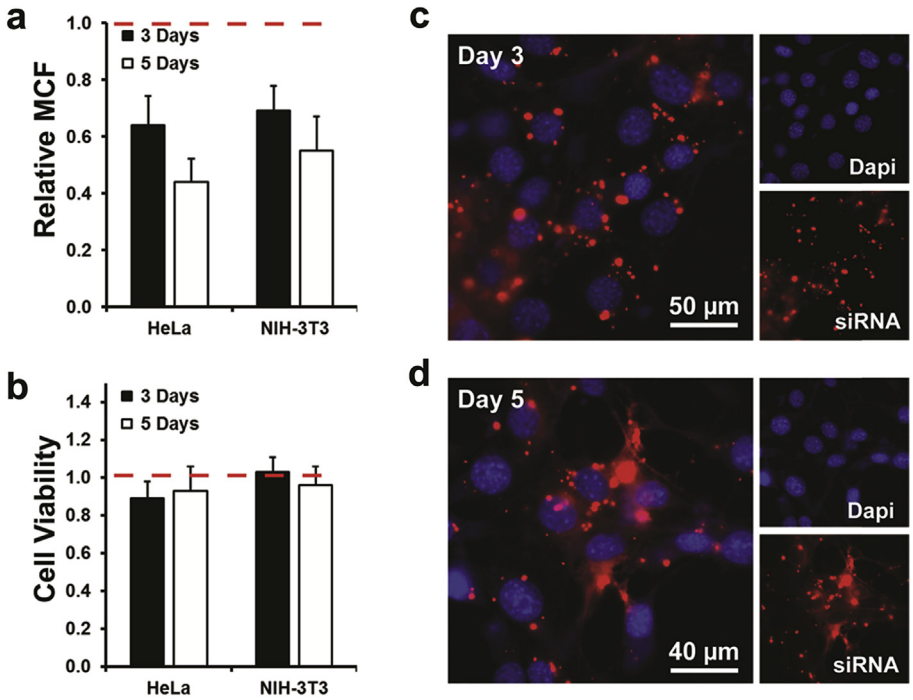

Fig. 3. *In vitro* evaluation of siRNA delivery from LbL coated sutures. (a) Flow cytometry analysis of mean cell fluorescence for HeLa and NIH-3T3 cells treated with siGFP containing LbL coated sutures relative to cells treated with siControl containing sutures. (b) Relative cell viability for cells treated with LbL coated sutures and those treated with uncoated sutures. (c) HeLa cell uptake of labeled siRNA film material after three days in culture. (d) HeLa cell uptake of labeled siRNA film material after five days in culture. Data shown are mean ± S.D., n = 3.

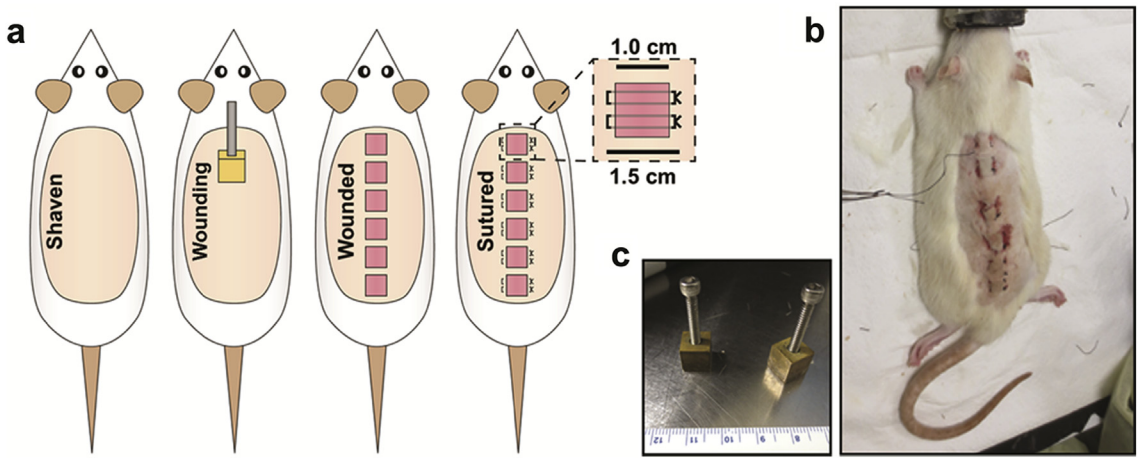

Fig. 4. The application of LbL coated sutures in a third-degree burn model in rats. (a) Cartoon schematic of the preparation the rats. Rats were shaven with an electric clipper, wounded with a heated (≥95 °C) brass block, and then four (4) sutures were placed laterally crossing the burn entering and exiting the dermis approximately 1–2 mm at the margin. (b) Image of the sutured rat post-operation closely resembles our goal. (c) Image of two of the brass blocks used to create burn injuries.

3.4. CTGF knockdown within burn wounds reduces contraction In vivo

Digital imaging of burn wounds was performed at the day of wounding, so called day 0, and after 15 and 30 days post-wounding (Fig. 5a). Grossly, the wounds are identical initially after wounding. The brass blocks create a uniform 1 cm [2] square burn that is only slightly obscured by suture placement. After 15 days the siCTGF wounds appear less contracted than either of the controls. Measuring the total scar area was complicated by the eschar having not fully released from some of the wounds (Fig. 5b). This issue was addressed by quantification of the scar area from analysis of digital wound images using ImageJ. The scar margin was determined from the hair line margins. After 15 days of treatment the scar area was significantly reduced in both siControl and uncoated suture treated wounds, indicating increased contraction within these burns compared to the siCTGF burns.

A key desired outcome of treatment is the lessening of the contraction that is characteristic of fibrotic wound closure. After 30 days of treatment the siCTGF treated scars appear significantly wider than the control treated burns, maintaining nearly twice the average scar width (Fig. 5c). Many of the control wounds appeared dramatically contracted, with a characteristic hourglass shape common to contracted scar. The total wound area in siCTGF treated wounds was approximately 167% that in burns treated with siControl sutures and 150% that of uncoated sutures. Interestingly it was observed that contraction within the siCTGF burns was particularly inhibited around the site of suture placement while regions of the scar far away from the suture appear significantly more contracted. This is distinct from what was observed in control

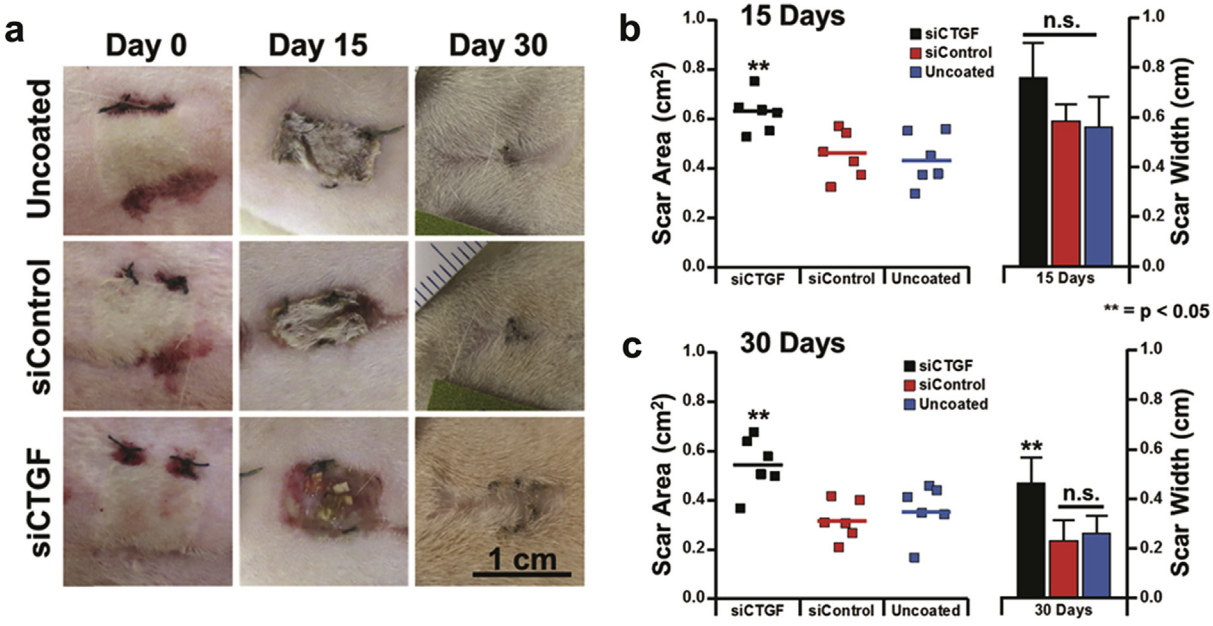

Fig. 5. Wound analysis by digital image quantification. (a) Representative digital images of wounds immediately after suture placement, after 15 days of treatment and after 30 days of treatment. (b) Quantification of wound images after 15 days. Both scar area and lateral width are elevated in the siCTGF wounds, indicating reduced contraction. (c) Quantification of wound images after 30 days of treatment. Both scar area and lateral width are elevated in the siCTGF wounds compared to controls, demonstrating significantly reduced contraction. Data shown are mean ± S.D., n = 6.

wounds, where the area of suture placement was where the highest degree of contraction was observed.

3.5. *In vivo silencing of CTGF and its effects on fibrosis related gene expression*

Connective tissue growth factor is a key mediator of the pro-fibrotic wound healing response to TGFβ signaling in cutaneous wound healing. Its expression *in vivo* has been previously connected to upregulated expression of a number of important proteins in scar production, including: alpha-smooth muscle actin (αSMA), tissue inhibitor of metalloproteinase-1 (TIMP-1), and collagen (Col1a1) (Fig. 6). It has been previously demonstrated that the knockdown of CTGF during dermal wound healing results in significantly reduced expression of these proteins and subsequently reduced local fibrosis. In this work we hypothesized that the controlled local delivery of siRNA targeting CTGF would have a similar response: by reducing local CTGF expression, we could also reduce the expression of these known downstream mediators of scar formation.

Gene expression was determined by qRT-PCR for mRNA expression in tissues isolated from within the sutured burn wounds, and compared to expression from unwounded dermis of the same rat. The expression of CTGF within the burn wound treated with siCTGF sutures was reduced by approximately 36% percent compared to controls after 30 days of treatment (Fig. 7a). CTGF expression was significantly elevated within all burn wounds when compared to the uninjured dermis; however, the relative level of upregulation was significantly different between the treatment groups. No difference was observed between the siControl and uncoated treatment groups.

Alpha smooth muscle actin is expressed by myofibroblasts within healing wounds, which act to drive wound contraction. For this reason, overexpression of αSMA within wounds is considered detrimental, as wound contraction often contributes to scar formation, poor tissue mobility, and subsequent functional impairments. Reduced αSMA expression has been previously demonstrated to reduce wound contraction in animal models and in *in vitro* studies. The expression of αSMA was significantly reduced within wounds treated with the siCTGF delivering sutures compared to either control group. Wounds treated with siControl containing sutures were observed to express αSMA at approximately 1.6 times that found in siCTGF treated wounds (Fig. 7b). This significant reduction in αSMA expression within the siCTGF treated wounds is likely one of the major contributing factors to the noticeably decreased wound contraction observed in these wounds.

Another important factor in scar formation is collagen production and its reorganization. Collagen is produced by fibroblasts within the healing tissue and is reorganized by matrix metalloproteinases (MMPs). The balance of collagen expression and MMP activity within a healing wound contributes significantly to the speed of healing and the quality of the tissue produced. It is known that upregulated MMP expression and activity along with lagging collagen production produces slow healing, poorly organized granulation tissue. In the case of scar formation this situation is reversed, and the overproduction of collagen and its gradual reorganization contribute to poor tissue function and scarring.

Importantly, CTGF overexpression within healing tissues is known to play an important role in TGFβ stimulated collagen production in cutaneous wound healing as well as its stimulation of TIMP1 expression. TIMP1 acts to inhibit MMPs that are crucial in the reorganization of dermal collagen. We found that in the case of siCTGF treated wounds, collagen and TIMP1 expression were both significantly reduced. Col1a1 was reduced by approximately 29% versus siControl wounds, while TIMP1 expression was reduced by approximately 23% (Fig. 7c–d).

4. Controlled siRNA delivery and knockdown of CTGF results in improved histological changes

Histological evaluation of treated scars was performed after 30 days of treatment. Wound sections were taken in the direction of suture placement from the center of each sutured burn wound and at two consecutive levels spaced 250 μm out from the center of the tissue. H&E histological analysis of the burn wounds focused primarily on tissue organization, scar characteristic dimensions, and general appearance. In H&E staining cutaneous scar tissue appears more cellular and has a less reticular tissue structure. Staining of the parenchyma is lighter in early scar tissue as compared to uninjured dermis. As the scar tissue matures and remodels the staining within the stroma increases to match the uninjured tissues. Beyond only staining, structural differences between uninjured tissue and scar tissue are dramatic and can be readily appreciated in H&E histology. Scar tissue lacks many of the natural structures found in the skin, including hair follicles, papillary structures, and sweat glands. The loss of these structures contributes to some of the complications of scar.

Qualitative analysis of the burn wounds demonstrated a number of noticeable differences between the siCTGF treated wounds and the control groups (Fig. 8a). The epidermal thickness of siCTGF wounds appeared increased in many of the wound sections, however it was not statistically significant when quantifies. Also concerning the epidermal layer of the skin, the first signs of papillary structures can be seen in siCTGF treated wounds. This is important as these structures are often lost in scar tissue and they function to improve the integration of the epidermis and the dermis, strengthening the bond between these layers of skin [73,74]. These structures were not seen in any of the control treated wounds. Another important observation to note was the epidermis was seen

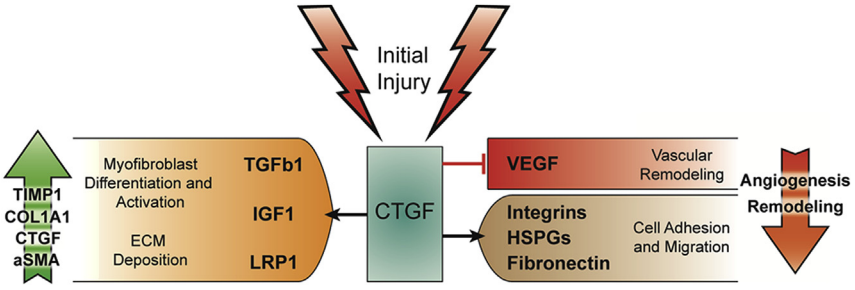

Fig. 6. Cartoon schematic of selected CTGF mediated pathways important in fibrosis. CTGF is known to mediate a number of diverse interactions between cell surface receptors, ECM proteins, and soluble growth factors and cytokines. These interactions influence a wide range of cellular behavior during wound healing.

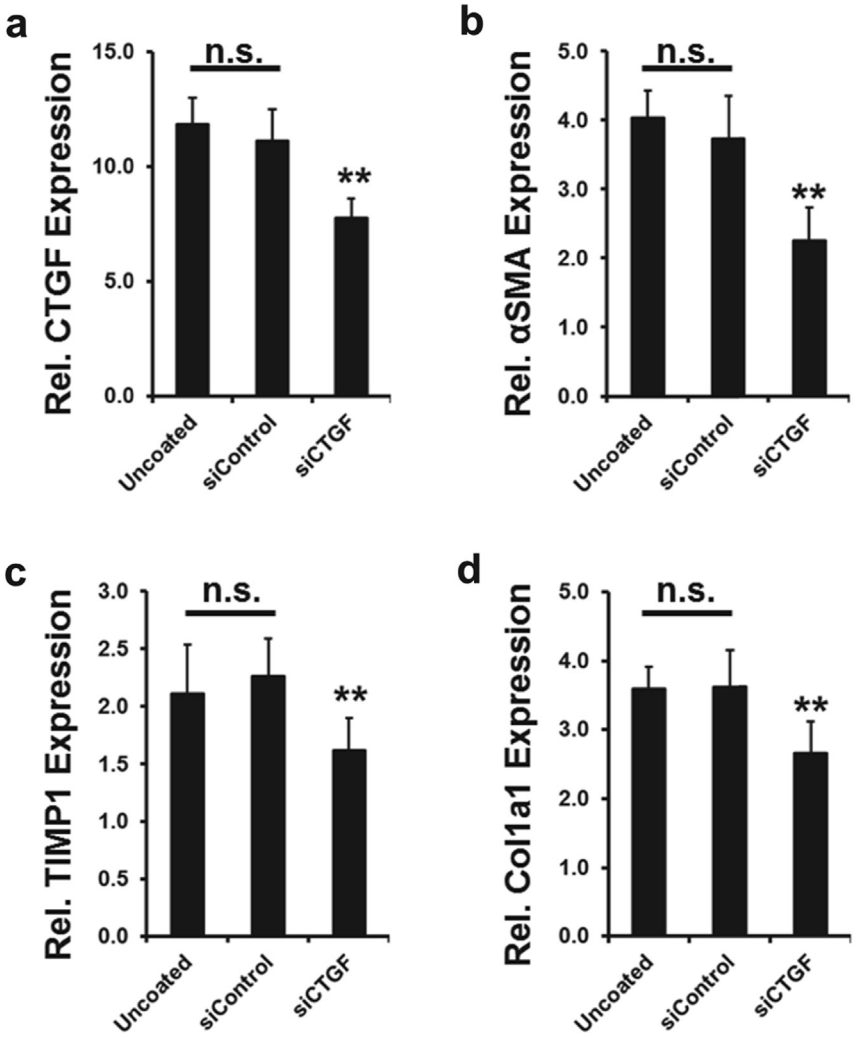

Fig. 7. Analysis of *in vivo* gene expression. (a) qRT-PCR analysis of CTGF expression in treated wounds relative to uninjured dermis from matched rats. (b) Relative expression of αSMA in treated wounds compared to uninjured dermis. (c) TIMP1expression in sutured wounds relative to uninjured dermis from matched rats. (d) Collagen expression within treated burn wounds relative to uninjured dermis. Data shown are mean ± S.D., n = 6.

to break free from the dermis within a number of the control wounds, demonstrating the lack of such a strong connection. The appearance of this junction in control wounds is flat with little variegation (Fig. 8b).

A common presentation in scars is hypertrophy, where the production of the healing tissue and wound contraction together lead to a scar that grows above the surrounding uninjured tissue. This presentation is very important to many of the aesthetic aspects of healing, as these raised scars can be undesirable. Grossly, we did not appreciate any significant hypertrophy within any of the burn wounds, and did not observe any correlation between treatment group and a raised or bumpy appearance. Histologically we observed this raised feature in a number of the treated wounds, however it was not consistently observed in any specific group. The relative vascularity of the scars was also of interest to us as good perfusion of the healing tissue is important to the overall health of the tissue. It has also been reported that CTGF may play a role in neovascularization [75–77]. To evaluate the impact on vascularity, we performed CD31 staining of wound sections and quantified both the number of vessels and average vessel diameter per high powered field. We found significantly increased vessel number in the siCTGF treated wounds with no observable differences between the control treated wounds. The average vessel diameter in all treatment groups was statistically similar (Sup. Fig 1).

As we had observed grossly, the siCTGF treated burns were wider than either the siControl or uncoated suture treated burns (Fig. 8c). The depth of the scar however is reduced by nearly half in the siCTGF treated wounds compared to controls (Fig. 8d). This dramatic reduction in scar depth is fascinating as it demonstrates the potential for improved long term reorganization of these wounds. Most of the siControl and uncoated suture treated burns were observed to have scars reaching down to skeletal muscle that could readily be identified in H&E staining after the 30 days of treatment. In the siCTGF burns, scars were far more topical, penetrating down to the skeletal muscle in small projections but not uniformly as seen in the control wounds. Overall, the appearance of the siCTGF treated burn wounds is much more remodeled than that seen in the control burns. This is evidenced by the presence of the darker staining parenchyma, which is more similar to uninjured dermis in appearance, within the scar body in the siCTGF treated wounds, while control burn wounds appear to uniformly consist of light staining scar tissue. This is a very promising finding in conjunction with the appearance of papillary structures in these burns, as the scar tissue treated with siCTGF sutures may be remodeling more effectively to recapitulate the uninjured dermis.

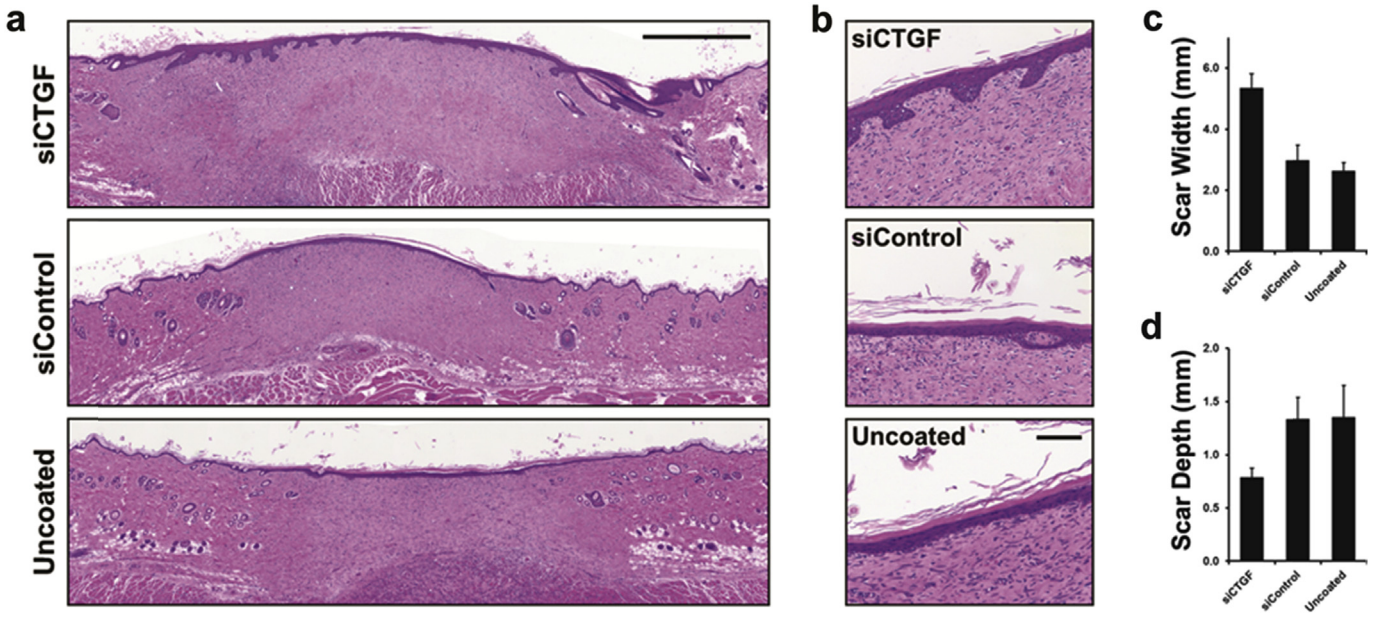

Fig. 8. H&E histology of scar tissue formation in treated burn wounds. (a) Representative full wound sections for each of the treatment groups. Scale bar = 1 mm. (b) High power images of the epidermis-dermis junction demonstrating papillary structures in siCTGF treated wounds that are absent in controls. Scale bar = 100 μm. (c) Average scar width as determined by histological analysis. (d) Average scar depth as determined from qualitative histological analysis. Data shown are mean ± S.D., n = 6.

4.1. Localized In vivo knockdown of CTGF improves tissue remodeling

Masson's trichrome stain (MTC) is an important connective tissue stain for analyzing collagen deposition within tissues. In the dermis, MTC stains collagen blue and cells, muscle, and keratin appear red. In healing tissue increases in collagen content can be appreciated in MTC stained sections for deeper staining blue color, while lower collagen content is a lighter shade of blue. Cellularity of tissues can also be appreciated, similar to H&E staining, as the cell body within the tissue appears red. This is particularly useful in identifying the epidermal layers as they stain a deep red with minimal blue staining. In MTC staining early scars are observed to stain lighter shade of blue than the uninjured dermis or healthy remodeled tissues due to the smaller size of the collagen fibers bundles within the scar and the relative increased cellularity.

Comparing the three treatment groups used in this work, MTC demonstrates a number of key differences between the siCTGF treated wounds and controls. Importantly, inspection of the full wound sections supports our previous findings from H&E histological analysis for increased scar width in the siCTGF burns (Fig. 9a). It also demonstrates increasing levels of reorganization within the healing scar. This can be appreciated in Fig. 9a by the dark blue staining regions crossing through the siCTGF scar. This increased staining above the skeletal muscle and through the scar demonstrates a significant level of remodeled tissue that appears much more similar to the uninjured dermis than the scars observed in the siControl or uncoated suture treated burns.

A second important finding observed in the MTC staining is the existence of papillary structures interconnecting the epidermis with the dermis (Fig. 9b). As we described in the previous section, these papillae serve to better integrate the epidermis with the dermis. Here we see that the epidermal tissue is well circumscribed and has a consistent variegated appearance. Inspecting the controls we see only a flat thin layer of cells lying on top of the dermis with no observable structures reaching into it from the epidermis. Looking closely at the border between the epidermis and dermis we can also appreciate the different organization of the dermal collagen. The collagen within the siCTGF treated wounds takes on a whirled reticular appearance, while the collagen seen to accumulate within the control treated wounds are flat up to and including this border region.

Grossly, the MTC stained full wound sections demonstrated increased tissue reorganization in the siCTGF treated wounds. This reorganizing is especially important at the wound margins to ensure a healthy integration of the healing tissue into the uninjured surrounding tissue. Qualitatively evaluating the scar margins of the different treatment groups we observe a number of important differences between them (Fig. 9c). Burns treated with siCTGF sutures have a less marked margin, obscured by large variations in the margin edge and regions of tissue that stain similarly to the uninjured dermis in the surrounding scar. Uncoated and siControl suture treated burns have fairly consistent clear margins with only small areas of remodeling at the margins.

4.2. Reduced total scar area and contraction

To evaluate collagen accumulation and organization further within the burn wound we used a second independent histological technique, picrosirius red (PS) staining of collagen. Collagen is a naturally birefringent macromolecule and as such can be readily evaluated using polarized light microscopy of histological sections. PS staining of collagen enhances this birefringence, allowing for more precise characterization collagen [78,79]. Histological analysis of PS stained tissues has been widely reported in the study of wound healing and scar formation to evaluate the extent and orientation of collagen present within the healing tissue [80]. In birefringence imaging thin Type III collagen has a blue-green appearance while thicker and more mature Type I collagen appears orange-red.

Here we use picrosirius red staining to evaluate the collagen content within burn wounds and the level of collagen orientation observed at the burn margin. Collagen content within scars is known to be increased. This collagen is often poorly organized and

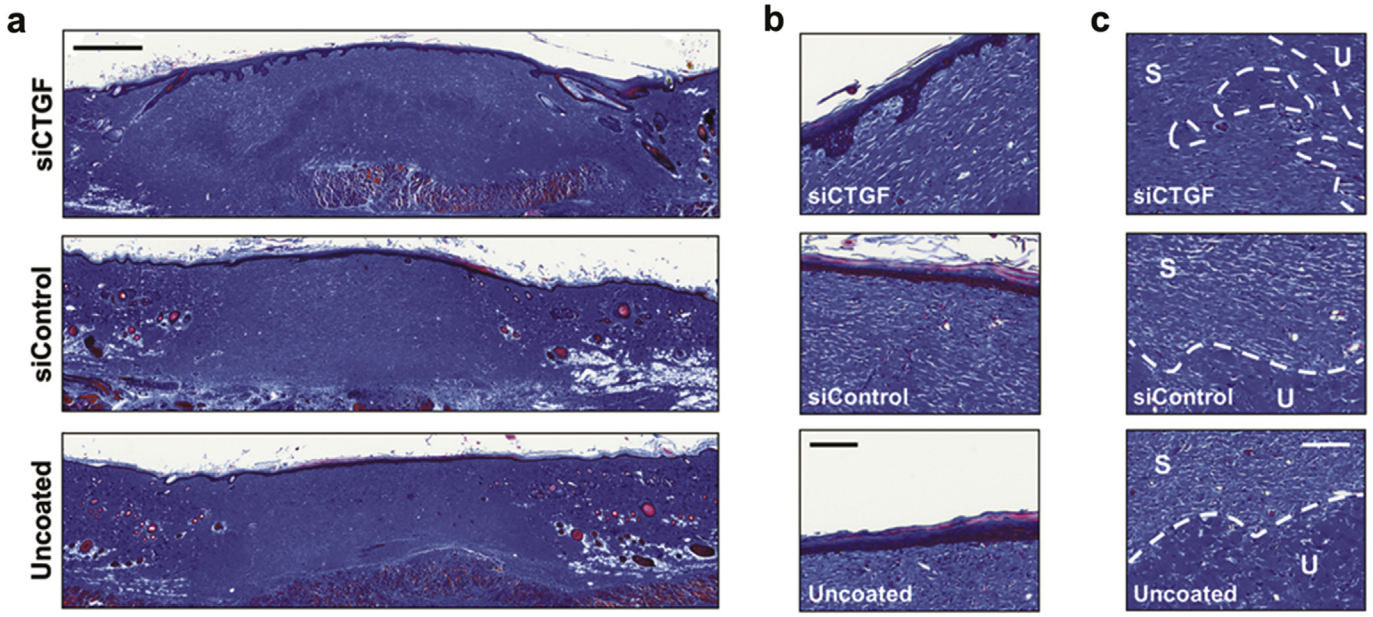

Fig. 9. Masson's trichrome staining of treated rat burn sections. (a) Representative full wound sections for gross histological comparison. Scale = 0.8 mm. (b) Representative high powered images of epidermal-dermal border demonstrating interdigitating epidermal papillae in siCTGF treated wounds not seen in controls. Scale bar = 100 μm (c) Representative high powered images of wound margins demonstrating the level of tissue reorganization observed in siCTGF treated wounds.

does not recapitulate the basket-weave structure that is observed in the uninjured dermis. Grossly analyzing the full wound sections, a dramatic difference between the siCTGF suture treated wounds and the siControl and uncoated suture treated wounds is easily apparent (Fig. 10a). The siCTGF scar region contains much larger collagen fibers that are evenly distributed and organized into a cross-hatching network. Similar to what we had observed in both H&E and MTC staining, the topical aspect of the scar is most consistent to the control wounds, however the depth of this region is less than half of that observed in the controls. It is also interesting to note here that regions we had noted were clearly scar tissue from H&E and MTC appear much more similar in collagen structure to the uninjured dermis than any such identifiable regions within the control burn wounds.

An important aspect of the pathology of scar tissue is contraction. Physiologically, contraction occurs as a result of mechanical forces

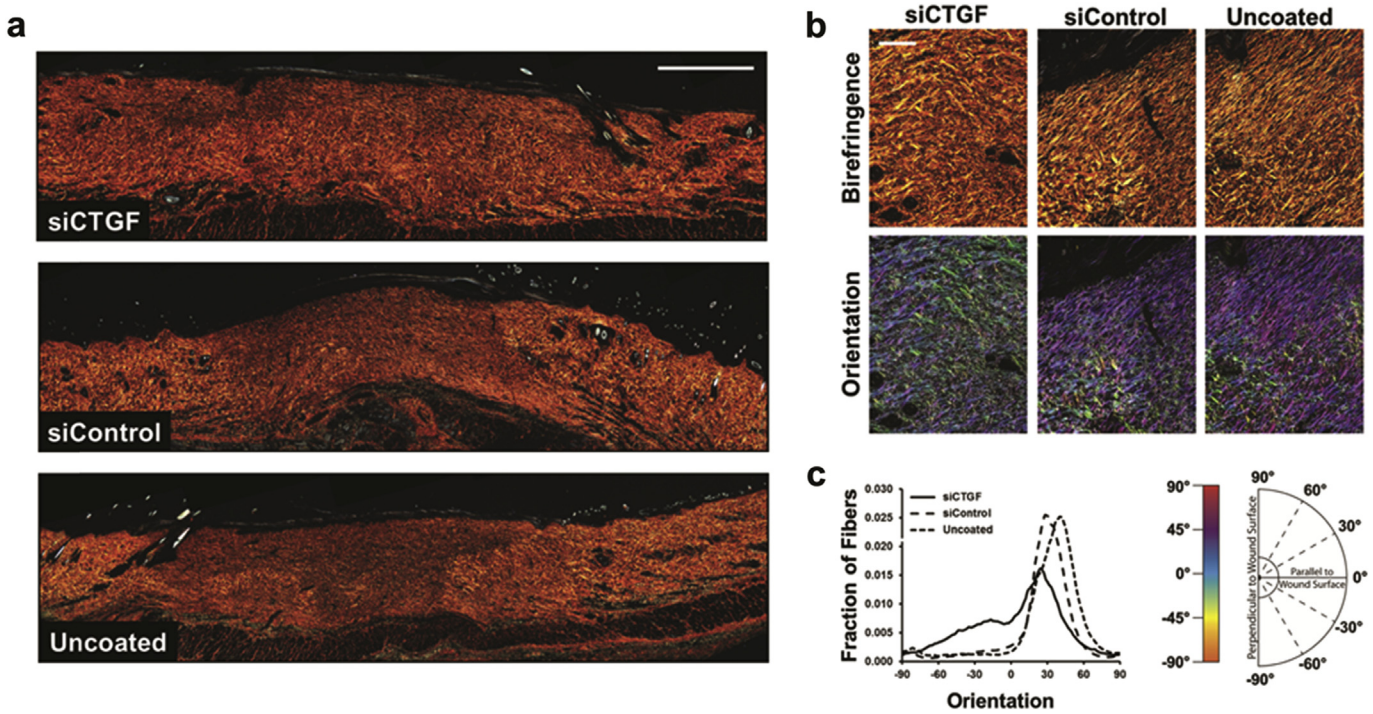

Fig. 10. Picrosirius red staining analysis of collagen content and orientation within the healing burn wounds. (a) Representative full wound sections imaged for birefringence for each treatment group. Scale bar = 1 mm. (b) Representative high power images of burn margins for each group and their respective orientation analysis color maps. Scale bar = 50 μm (c) Plot of average fiber orientation fractions for each treatment group. Data shown are mean, n = 4.

transmitted across the ECM within the scar. Collagen is a primary component of that ECM. Orientation of collagen fibers is an important factor in evaluating scar characteristics as it gives insight into the level of mechanical force being transmitted across the fibers. Highly aligned collagen in the orientation of contraction, which in this animal model would be laterally across the wound sections, helps characterize the level of contraction ongoing within the scar.

Here we performed orientation analysis of the large to medium collagen fibers at the scar margin to assess the extent of contraction within these wounds, performed using the ImageJ plugin OrientationJ [81]. This analysis demonstrates the high degree of orientation with the collagen fibers at the scar margin of siControl and uncoated suture treated burns. The siCTGF treated burns however demonstrate significantly less alignment, and have a much more woven characteristic to their appearance. This is important as it demonstrates the extent to which contractile forces are present within the control wounds, and how they are still present in the siCTGF treated wounds, but to a lesser degree. In the color maps the purple-blue shaded collagen fibers are oriented in the direction of the scar center and are abundant in the control wounds. These fibers are visible within the siCTGF treated burn but not to the same degree and mixed in with a substantial population of fibers seen going in opposing directions (Fig. 10b–c).

5. Discussion

Scars are an everyday part of life, but in the case of large traumatic injuries, burns, and surgery, they can create a great deal of discomfort for patients both physically and aesthetically [2,7,8]. Specifically, in the case of burn wounds, contractions can lead to serious complications including range of motion issues and loss of function for the tissues involved [6,82]. These issues become key to both quality of life and function, and affect a range of patients, from childhood burn victims to soldiers on the battlefield suffering large traumatic injuries. The current treatment options available to patients largely consist of silicone gel sheeting and topical steroids, which can slow wound healing and increase the risk of serious infection [7]. To date a great deal of research has been done to identify key biological mediators of scar production, however being able to specifically target these actors has been limited due to the lack of technology to effectively deliver targeted therapies locally at the site of interest. In this report we describe using a layer-by-layer assembled thin film platform for the localized delivery of RNAi from as one approach to this goal.

In this report we describe the application of an ultrathin polymer film coating for the sustained local delivery of siRNA into healing third-degree burns in a rat model. We used a commercially available silk suture coated with the LbL film which could be placed through the burn wound to provide an siRNA delivery depot within the healing tissue. Here we targeted a known mediator of TGFβ stimulated fibrosis, connective tissue growth factor. CTGF is known to be upregulated within hypertrophic scars and its expression is associated with the increased expression of collagen, TIMP1, and alpha-smooth muscle actin within scars. Previous reports have demonstrated that anti-sense RNA therapy against CTGF expression within wounds leads to reduced scar production. These reports, however, have focused on the bolus administration of RNA to the wound site, leaving the RNA open to rapid clearance and poor bioavailability, thus achieving lower potential efficacies. Using LbL coatings to sustain the local delivery of siRNA into the healing wound is an approach that we believe addresses both of these concerns. In this work we demonstrate how one might approach the controlled delivery of siRNA from a coated substrate common in the wound sites where scars form, targeting this key mediator which resulted in significant changes in scar formation in a third-degree burn model in rats.

Ultrathin coatings were observed to uniformly coat the surfaces of commercially available silk sutures and were demonstrated to sustain the release of siRNA out to nearly two weeks. These film coated sutures were tested for *in vitro* siRNA-specific gene knockdown and were shown to reduce the expression of the reporter gene GFP in two different cell lines for up to five days with minimal impact on cell viability. This film coated suture when placed through third-degree burn wounds was able to achieve significant siRNA-specific reduction of CTGF expression *in vivo*. This reduction in CTGF expression was connected to reduced expression of many related TGFβ stimulated pro-fibrotic genes, including collagen, TIMP1, and αSMA. Macroscopically siCTGF treated wounds were significantly less contracted than wounds treated with either siControl coated sutures or uncoated sutures.

Histologically the siCTGF scars were significantly less contracted than control scars, and were significantly shallower. The healed tissue within the siCTGF treated burn wound contained papillary structures, which play a crucial role in providing a strong connection between the epidermis and the dermis. These structures were not observed in any of the control scars. In addition to these findings, the level of remodeling within the siCTGF treated wounds was also increased compared to controls. MTC staining of wound sections provided evidence of increased reorganization of the healing tissue and more advanced remodeling of the scar margins. Finally, picrosirius red staining of the treated wound sections provided a great deal of insight into the organization of collagen within the healing tissues and the level of contractile forces acting on them. It was observed that reducing CTGF expression improved collagen remodeling within the burn wound and significantly reduced the level of collagen orientation at the scar margin, indicating significantly reduced contractile forces within the tissue.

In summary, we have presented the local application of an ultrathin polymer coating that can be uniformly assembled onto a commercially available suture for the sustained effective knockdown of a key mediator in cutaneous scar formation *in vivo*. This targeted therapy resulted in a significantly reduced fibrotic response within healing burn tissue. The work detailed in this report is one of the first demonstrations of controlled local RNA delivery into healing burns to improve outcomes. This work also substantiates the previously reported findings that CTGF is a potential therapeutic target within wounds to reduce fibrosis while not impairing normal wound healing. The approach outlined within this report has the potential to significantly impact a myriad of diverse fields, from treating liver, renal, and pulmonary fibrosis to developing regenerative medicines, cancer therapies, and providing a tool in fundamental scientific research.

Author Contributions

S.C. and performed surgeries and experiments, collected and analyzed data, and wrote the manuscript. A.G., S.K., and M.S. assisted in surgeries and helped write the manuscript. B.A. assisted in experiments. W.A., M.Y., and P.H. developed and supervised the project. The manuscript was read and approved by all co-authors.

Competing financial interests

The authors declare no competing financial interests.

Acknowledgments

This research was supported in part by funding and core facilities provided by the U.S. Army Research Office under contract W911NF-07-D-0004 at the MIT Institute of Soldier

Nanotechnology. We acknowledge Shriners Grant #85120-BOS for the support of this study. This work was also supported by use of core facilities at the Koch Institute for Integrative Cancer Research (supported by the NCI under grant 2P30CA014051-39). We thank the Koch Institute Swanson Biotechnology Center for technical support, specifically the microscopy, flow cytometry, and histology cores. The authors wish to dedicate this paper to the memory of Officer Sean Collier, for his caring service to the MIT community and for his sacrifice.

Appendix A. Supplementary data

Supplementary data related to this article can be found at http://dx.doi.org/10.1016/j.biomaterials.2016.04.007.

References

[1] R. Baker, F. Urso-Baiarda, C. Linge, A. Grobbelaar, Cutaneous scarring: a clinical review, Dermatol Res. Pract. 2009 (2009) 625376.
[2] T.A. Mustoe, Scars and keloids, Bmj 328 (2004) 1329–1330.
[3] A.D. Widgerow, L.A. Chait, Scar management practice and science: a comprehensive approach to controlling scar tissue and avoiding hypertrophic scarring, Adv. Skin. Wound Care 24 (2011) 555–561.
[4] G.C. Gurtner, S. Werner, Y. Barrandon, M.T. Longaker, Wound repair and regeneration, Nature 453 (2008) 314–321.
[5] G.C. Gurtner, R.J. Rohrich, M.T. Longaker, From bedside to bench and back again: technology innovation in plastic surgery, Plast. Reconstr. Surg. 124 (2009) 1355–1356.
[6] B. Nedelec, A. Ghahary, P.G. Scott, E.E. Tredget, Control of wound contraction. Basic and clinical features, Hand Clin. 16 (2000) 289–302.
[7] T.A. Mustoe, et al., International clinical recommendations on scar management, Plast. Reconstr. Surg. 110 (2002) 560–571.
[8] T.A. Mustoe, Evolution of silicone therapy and mechanism of action in scar management, Aesthet. Plast. Surg. 32 (2008) 82–92.
[9] G.G. Walmsley, et al., Scarless wound healing: chasing the holy grail, Plast. Reconstr. Surg. 135 (2015) 907–917.
[10] V.W. Wong, G.C. Gurtner, M.T. Longaker, Wound healing: a paradigm for regeneration, Mayo Clin. Proc. 88 (2013) 1022–1031.
[11] A. Nauta, G. Gurtner, M.T. Longaker, Wound healing and regenerative strategies, Oral Dis. 17 (2011) 541–549.
[12] J.E. Park, A. Barbul, Understanding the role of immune regulation in wound healing, Am. J. Surg. 187 (2004) 11S–16S.
[13] R. Goldschmeding, et al., Connective tissue growth factor: just another factor in renal fibrosis? Nephrol. Dial. Transpl. 15 (2000) 296–299.
[14] W.A. Border, D. Brees, N.A. Noble, Transforming growth factor-beta and extracellular matrix deposition in the kidney, Contrib. Nephrol. 107 (1994) 140–145.
[15] W.A. Border, N.A. Noble, Transforming growth factor beta in tissue fibrosis, N. Engl. J. Med. 331 (1994) 1286–1292.
[16] H. Birkedal-Hansen, Proteolytic remodeling of extracellular matrix, Curr. Opin. Cell Biol. 7 (1995) 728–735.
[17] F. Grinnell, Fibroblasts, myofibroblasts, and wound contraction, J. Cell Biol. 124 (1994) 401–404.
[18] R.J. Mackool, G.K. Gittes, M.T. Longaker, Scarless healing. The fetal wound, Clin. Plast. Surg. 25 (1998) 357–365.
[19] C.K. Sen, et al., Human skin wounds: a major and snowballing threat to public health and the economy, Wound Repair Regen. 17 (2009) 763–771.
[20] C.L. Rock, R.E. Dechert, R. Khilnani, R.S. Parker, J.L. Rodriguez, Carotenoids and antioxidant vitamins in patients after burn injury, J. Burn Care Rehabil. 18 (1997) 269–278 discussion 268.
[21] A.H. DeCherney, et al., Expression of cyclin protein after thermal skin injury in a guinea pig model, J. Burn Care Rehabil. 18 (1997) 292–298.
[22] K.E. Rodgers, et al., Histologic alterations in dermal repair after thermal injury effects of topical angiotensin II, J. Burn Care Rehabil. 18 (1997) 381–388.
[23] J.F. Fraser, et al., Deep dermal burn injury results in scarless wound healing in the ovine fetus, Wound Repair Regen. 13 (2005) 189–197.
[24] J.W. Penn, A.O. Grobbelaar, K.J. Rolfe, The role of the TGF-beta family in wound healing, burns and scarring: a review, Int. J. Burns Trauma 2 (2012) 18–28.
[25] R.A. Pena, J.A. Jerdan, B.M. Glaser, Effects of TGF-beta and TGF-beta neutralizing antibodies on fibroblast-induced collagen gel contraction: implications for proliferative vitreoretinopathy, Invest. Ophthalmol. Vis. Sci. 35 (1994) 2804–2808.
[26] M.F. Cordeiro, et al., Novel antisense oligonucleotides targeting TGF-beta inhibit in vivo scarring and improve surgical outcome, Gene Ther. 10 (2003) 59–71.
[27] S.M. Wahl, Transforming growth factor beta (TGF-beta) in inflammation: a cause and a cure, J. Clin. Immunol. 12 (1992) 61–74.
[28] S. O'Kane, M.W. Ferguson, Transforming growth factor beta s and wound healing, Int. J. Biochem. Cell Biol. 29 (1997) 63–78.
[29] W.A. Border, Transforming growth factor-beta and the pathogenesis of glomerular diseases, Curr. Opin. Nephrol. Hypertens. 3 (1994) 54–58.
[30] W.A. Border, N.A. Noble, TGF-beta in kidney fibrosis: a target for gene therapy, Kidney Int. 51 (1997) 1388–1396.
[31] R. Montesano, L. Orci, Transforming growth factor beta stimulates collagen-matrix contraction by fibroblasts: implications for wound healing, Proc. Natl. Acad. Sci. U. S. A. 85 (1988) 4894–4897.
[32] J. Massague, D. Wotton, Transcriptional control by the TGF-beta/Smad signaling system, Embo J. 19 (2000) 1745–1754.
[33] A. Desmouliere, A. Geinoz, F. Gabbiani, G. Gabbiani, Transforming growth factor-beta 1 induces alpha-smooth muscle actin expression in granulation tissue myofibroblasts and in quiescent and growing cultured fibroblasts, J. Cell Biol. 122 (1993) 103–111.
[34] M.H. Branton, J.B. Kopp, TGF-beta and fibrosis, Microbes Infect. 1 (1999) 1349–1365.
[35] M. Sisco, et al., Antisense oligonucleotides against transforming growth factor-beta delay wound healing in a rabbit ear model, J. Am. Coll. Surg. 201 (2005). S60–S60.
[36] K.E. Lipson, C. Wong, Y. Teng, S. Spong, CTGF is a central mediator of tissue remodeling and fibrosis and its inhibition can reverse the process of fibrosis, Fibrogenes. Tissue Repair 5 (2012) S24.
[37] X. Wang, S.V. McLennan, T.J. Allen, S.M. Twigg, Regulation of pro-inflammatory and pro-fibrotic factors by CCN2/CTGF in H9c2 cardiomyocytes, J. Cell Commun. Signal 4 (2010) 15–23.
[38] D.W. Esson, et al., Expression of connective tissue growth factor after glaucoma filtration surgery in a rabbit model, Invest. Ophthalmol. Vis. Sci. 45 (2004) 485–491.
[39] J. Dammeier, M. Brauchle, W. Falk, G.R. Grotendorst, S. Werner, Connective tissue growth factor: a novel regulator of mucosal repair and fibrosis in inflammatory bowel disease? Int. J. Biochem. Cell Biol. 30 (1998) 909–922.
[40] M.R. Duncan, et al., Connective tissue growth factor mediates transforming growth factor beta-induced collagen synthesis: down-regulation by cAMP, FASEB J. Off. Publ. Fed. Am. Soc. Exp. Biol. 13 (1999) 1774–1786.
[41] E. Gore-Hyer, et al., TGF-beta and CTGF have overlapping and distinct fibrogenic effects on human renal cells, Am. J. Physiol. Ren. Physiol. 283 (2002) F707–F716.
[42] G.R. Grotendorst, Connective tissue growth factor: a mediator of TGF-beta action on fibroblasts, Cytokine Growth Factor Rev. 8 (1997) 171–179.
[43] A. Igarashi, H. Okochi, D.M. Bradham, G.R. Grotendorst, Regulation of connective tissue growth factor gene expression in human skin fibroblasts and during wound repair, Mol. Biol. Cell 4 (1993) 637–645.
[44] J.G. Abreu, N.I. Ketpura, B. Reversade, E.M. De Robertis, Connective-tissue growth factor (CTGF) modulates cell signalling by BMP and TGF-beta, Nat. Cell Biol. 4 (2002) 599–604.
[45] A. Holmes, et al., CTGF and SMADs, maintenance of scleroderma phenotype is independent of SMAD signaling, J. Biol. Chem. 276 (2001) 10594–10601.
[46] Y. Ito, et al., Expression of connective tissue growth factor in human renal fibrosis, Kidney Int. 53 (1998) 853–861.
[47] A. Leask, A. Holmes, C.M. Black, D.J. Abraham, Connective tissue growth factor gene regulation. Requirements for its induction by transforming growth factor-beta 2 in fibroblasts, J. Biol. Chem. 278 (2003) 13008–13015.
[48] A. Leask, et al., The control of ccn2 (ctgf) gene expression in normal and scleroderma fibroblasts, Mol. Pathol. 54 (2001) 180–183.
[49] R.A. Ignotz, J. Massague, Transforming growth-factor-beta stimulates the expression of Fibronectin and collagen and their incorporation into the extracellular-matrix, J. Biol. Chem. 261 (1986) 4337–4345.
[50] H. Yokoi, et al., Role of connective tissue growth factor in profibrotic action of transforming growth factor-beta: a potential target for preventing renal fibrosis, Am. J. Kidney Dis. 38 (2001) S134–S138.
[51] K. Frazier, S. Williams, D. Kothapalli, H. Klapper, G.R. Grotendorst, Stimulation of fibroblast cell growth, matrix production, and granulation tissue formation by connective tissue growth factor, J. Invest. Dermatol. 107 (1996) 404–411.
[52] H. Okada, et al., Connective tissue growth factor expressed in tubular epithelium plays a pivotal role in renal fibrogenesis, J. Am. Soc. Nephrol. 16 (2005) 133–143.
[53] Y.T. Khoo, et al., Upregulation of secretory connective tissue growth factor (CTGF) in keratinocyte-fibroblast coculture contributes to keloid pathogenesis, J. Cell Physiol. 208 (2006) 336–343.
[54] J.T. Daniels, et al., Understanding and controlling the scarring response: the contribution of histology and microscopy, Microsc. Res. Tech. 42 (1998) 317–333.
[55] H. Washio, et al., Transcriptional inhibition of hypertrophic scars by a gene silencer, pyrrole-imidazole polyamide, targeting the TGF-beta1 promoter, J. Invest. Dermatol. 131 (2011) 1987–1995.
[56] K.D. O'Shaughnessy, P. Kim, N.K. Roy, T.A. Mustoe, Antisense oligonucleotides to TGF-beta and CTGF decrease hypertrophic scarring in a rabbit ear model, Wound Repair Regen. 15 (2007). A20–A20.
[57] M. Sisco, et al., Antisense inhibition of connective tissue growth factor (CTGF/CCN2) mRNA limits hypertrophic scarring without affecting wound healing in vivo, Wound Repair Regen. 16 (2008) 661–673.
[58] S. Sriram, P. Robinson, L. Pi, A.S. Lewin, G. Schultz, Triple combination of siRNAs targeting TGFbeta1, TGFbetaR2, and CTGF enhances reduction of collagen I and smooth muscle actin in corneal fibroblasts, Invest. Ophthalmol. Vis. Sci. 54 (2013) 8214–8223.
[59] D.J. Gibson, et al., Conditional knockout of CTGF affects corneal wound healing, Invest. Ophthalmol. Vis. Sci. 55 (2014) 2062–2070.

[60] J.K. Crean, D. Lappin, C. Godson, H.R. Brady, Connective tissue growth factor: an attractive therapeutic target in fibrotic renal disease, Expert Opin. Ther. Targets 5 (2001) 519–530.
[61] K.C. Wood, J.Q. Boedicker, D.M. Lynn, P.T. Hammond, Tunable drug release from hydrolytically degradable layer-by-layer thin films, Langmuir ACS J. Surf. Colloids 21 (2005) 1603–1609.
[62] K.C. Wood, H.F. Chuang, R.D. Batten, D.M. Lynn, P.T. Hammond, Controlling interlayer diffusion to achieve sustained, multiagent delivery from layer-by-layer thin films, Proc. Natl. Acad. Sci. U. S. A. 103 (2006) 10207–10212.
[63] G. Decher, Fuzzy nanoassemblies: toward layered polymeric multicomposites, Science 277 (1997) 1232–1237.
[64] G. Decher, et al., Layer-by-Layer adsorbed films of polyelectrolytes, proteins or DNA, Abstr. Pap. Am. Chem. S 205 (1993), 334–POLY.
[65] P.T. Hammond, Building biomedical materials layer-by-layer, Mater. Today 15 (2012) 196–206.
[66] A. Golberg, et al., Non-thermal, pulsed electric field cell ablation: a novel tool for regenerative medicine and scarless skin regeneration, Technol. (Singap. World Sci.) 1 (2013) 1–8.
[67] A. Golberg, et al., Pulsed electric fields for burn wound disinfection in a murine model, J. Burn Care Res. 36 (2015) 7–13.
[68] A. Golberg, et al., Eradication of multidrug-resistant in burn wounds by antiseptic pulsed electric field, Technol. (Singap. World Sci.) 2 (2014) 153–160.
[69] M.P. Alfaro, et al., A physiological role for connective tissue growth factor in early wound healing, Lab. Invest. 93 (2013) 81–95.
[70] J.F. Wang, et al., Fibrocytes from burn patients regulate the activities of fibroblasts, Wound Repair Regen. 15 (2007) 113–121.
[71] D.M. Lynn, R. Langer, Degradable poly(beta-amino esters): synthesis, characterization, and self-assembly with plasmid DNA, J. Am. Chem. Soc. 122 (2000) 10761–10768.
[72] S. Castleberry, M. Wang, P.T. Hammond, Nanolayered siRNA dressing for sustained localized knockdown, ACS Nano 7 (2013) 5251–5261.
[73] C.M. Lin, et al., Microencapsulated human hair dermal papilla cells: a substitute for dermal papilla? Arch. Dermatol. Res. 300 (2008) 531–535.
[74] K. Elliott, T.J. Stephenson, A.G. Messenger, Differences in hair follicle dermal papilla volume are due to extracellular matrix volume and cell number: implications for the control of hair follicle size and androgen responses, J. Invest. Dermatol. 113 (1999) 873–877.
[75] S. Kondo, et al., Connective tissue growth factor increased by hypoxia may initiate angiogenesis in collaboration with matrix metalloproteinases, Carcinogenesis 23 (2002) 769–776.
[76] G. Hashimoto, et al., Matrix metalloproteinases cleave connective tissue growth factor and reactivate angiogenic activity of vascular endothelial growth factor 165, J. Biol. Chem. 277 (2002) 36288–36295.
[77] I. Inoki, et al., Connective tissue growth factor binds vascular endothelial growth factor (VEGF) and inhibits VEGF-induced angiogenesis, FASEB J. Off. Publ. Fed. Am. Soc. Exp. Biol. 16 (2002) 219–221.
[78] L.C. Junqueira, W. Cossermelli, R. Brentani, Differential staining of collagens type I, II and III by Sirius Red and polarization microscopy, Arch. Histol. Jpn. 41 (1978) 267–274.
[79] G.S. Montes, L.C. Junqueira, The use of the Picrosirius-polarization method for the study of the biopathology of collagen, Mem. Inst. Oswaldo Cruz 86 (Suppl 3) (1991) 1–11.
[80] L. Cuttle, et al., Collagen in the scarless fetal skin wound: detection with picrosirius-polarization, Wound Repair Regen. 13 (2005) 198–204.
[81] R. Rezakhaniha, et al., Experimental investigation of collagen waviness and orientation in the arterial adventitia using confocal laser scanning microscopy, Biomech. Model Mechanobiol. 11 (2012) 461–473.
[82] J.T. Daniels, et al., Mediation of transforming growth factor-beta(1)-stimulated matrix contraction by fibroblasts: a role for connective tissue growth factor in contractile scarring, Am. J. Pathol. 163 (2003) 2043–2052.